



CrossMark
click for updates

Cite this: *RSC Adv.*, 2016, 6, 51456

Hydrogen bonding interactions affect the hierarchical self-assembly and secondary structures of comb-like polypeptide supramolecular complexes displaying photoresponsive behavior†

Mohamed Gamal Mohamed,^a Jia-Huei Tu,^a Shih-Hung Huang,^a Yeo-Wan Chiang^a and Shiao-Wei Kuo^{*ab}

In this study we blended 4-(4-hexadecylphenylazo)pyridine (AzoPy-C16), synthesized through facile diazonium and monoetherification reactions, with polytyrosine (PTyr) to form comb-like polypeptide supramolecular complexes stabilized through hydrogen bonding between the pyridyl ring of each AzoPy-C16 unit and the OH groups of PTyr. The secondary structure of PTyr transformed from an α -helical to a β -sheet conformation upon the addition of AzoPy-C16, because the long alkyl chains of the AzoPy-C16 units disrupted the weak intramolecular hydrogen bonds between the C=O and NH groups in the α -helical conformation, as determined using Fourier transform infrared (FTIR) and circular dichroism (CD) spectroscopy. Small-angle X-ray scattering (SAXS) and wide-angle X-ray diffraction (WAXD) suggested a hierarchical lamellae-within-lamellae structure for the PTyr/AzoPy-C16 supramolecular complex, featuring long-range-ordered lamellae arising from the antiparallel β -pleated sheet conformation of PTyr ($d = 1.15$ nm) within long-range-ordered lamellae arising from the alkyl groups of AzoPy-C16 units ($d = 5.94$ nm), oriented in a perpendicular manner. The d -spacing and long-range order of the lamellar structure formed from the alkyl groups decreased upon UV irradiation as the rod-like *trans* isomers of the AzoPy-C16 units transformed into V-shaped *cis* counterparts. This phenomenon also led to a change in the water contact angle of the supramolecular material, with the hydrophobic surface of PTyr/*trans*-AzoPy-C16 (94.2°) transforming to a hydrophilic surface for PTyr/*cis*-AzoPy-C16 (61.3°).

Received 27th March 2016
Accepted 16th May 2016

DOI: 10.1039/c6ra07907e

www.rsc.org/advances

Introduction

Polypeptides, amino acid-based biopolymers, have attracted much attention because of their potential applications as, for example, responsive materials for biosensors and matrices for gene and drug delivery.^{1–10} Polypeptides can fold into several well-defined secondary structures; for example, rigid rod-like structures (α -helical conformations) originating mainly from strong intramolecular hydrogen bonding between oxygen atoms of carbonyl groups (C=O) and hydrogen atoms of amide groups (NH–C=O) in the main chain backbones of polypeptides, and β -sheet conformations stabilized through intermolecular hydrogen bonding interactions of peptide groups.^{11–17} The conformational

changes of polypeptides are strongly dependent on the solvent polarity or quality, which can influence the formation of intramolecular hydrogen bonds. For example, when poly[*N*⁵-(2-hydroxyethyl)-*L*-glutamine] is dissolved in alcohol, water, or water/alcohol mixtures, the secondary structure can change from a rod-like α -helix to a flexible random coil.^{18,19} The synthesis of polypeptides having well-defined secondary structures (α -helices or β -sheets) can be performed through controlled/living ring-opening polymerization of amino acid *N*-carboxyanhydrides (NCAs). The advantages of NCA polymerization are controlled large-scale preparation, controlled molecular weight of the polypeptide, and the ability to combine polypeptides with different architectures (*e.g.*, dendrimers, block copolymers, star-shaped polymers, graft copolymers, random copolymers).^{20–23}

Azobenzene is a commonly used photochromic molecule that undergoes reversible *trans*–*cis* photoisomerization upon irradiation with UV light (350 nm).^{24–26} In this present study we used an azopyridine (AzoPy) derivative presenting a long alkyl chain as a type of azobenzene capable of undergoing such photoisomerization as well as self-assembling with organic acids through the formation of hydrogen bonds with its pyridyl group.

^aDepartment of Materials and Optoelectronic Science, Center for Functional Polymers and Supramolecular Materials, National Sun Yat-Sen University, Kaohsiung, Taiwan. E-mail: kuosw@faculty.nsysu.edu.tw

^bDepartment of Medicinal and Applied Chemistry, Kaohsiung Medical University, Kaohsiung, Taiwan

† Electronic supplementary information (ESI) available. See DOI: 10.1039/c6ra07907e

The photoisomerization ability of AzoPy suggests that it has several potential applications in photonics, photo-driven devices, and flat-panel displays.^{27–33} For example, Lu *et al.* constructed photoresponsive halogen-bonded liquid crystals featuring ionic bonds between halogen atoms and AzoPy molecules; these liquid-crystalline materials underwent photoinduced phase transitions upon irradiation with UV light.²⁸ The same group also reported various fiber morphologies upon the supramolecular self-organization of AzoPy with inorganic acids and organic solvents, stabilized through halogen and hydrogen bonds.³¹ Kawatsuki *et al.* used reversible-fragmentation chain transfer (RAFT) polymerization to synthesize diblock and random copolymers of poly[(2-trifluoroethylmethacrylate)-*co*-(methacrylic acid)] presenting carboxyl groups (COOH) from their side chains; films of these materials exhibited green fluorescence when blended with a fluorene derivative presenting a pyridine ring, the result of stabilizing hydrogen bonding interactions.³⁴ Kobayashi *et al.* fabricated photoresponsive supramolecular liquid-crystalline polymer microparticles through a facile phase reversion method with hydrogen bonds formed between the free pyridyl units of a homopolymer and dicarboxylic acid molecules.³⁵

The noncovalent interactions used to form supramolecular structures are typically hydrogen bonding, π - π stacking, ionic, metal-ligand, and hydrophobic interactions.^{35–40} The secondary structures of polypeptides can, for example, be tuned or controlled simply through varying the strength of hydrogen bonding interactions. Indeed, we have found that blending poly(γ -ethyl L-glutamate), poly(γ -methyl-L-glutamate), and poly(γ -benzyl-L-glutamate) with random-coil oligomers [e.g., poly(vinylphenol) (PVPh), phenolic resin] can lead to stabilization of their helical conformations as a result of relatively strong intermolecular hydrogen bonds between the C=O groups on the side chains of the polypeptides and the OH groups of PVPh/phenolic resin.^{41,42} In addition, when we blended a low-molecular-weight polytyrosine (PTyr) with a random-coil homopolymer (P4VP) in two different solvents [methanol (MeOH), dimethylformamide (DMF)], the glass transition temperatures (T_g) of the PTyr/P4VP supramolecular complexes obtained from the MeOH solution were higher than those of the PTyr/P4VP blend, mainly because of the formation of interpolymer complex aggregates.⁴² Recently, we prepared a 2,4,6-triphenylpyridine-functionalized polytyrosine (pyridine-PTyr) through ring-opening polymerization of Tyr-NCA at room temperature; according to wide-angle X-ray diffraction (WAXD) analysis, the β -sheet conformation of pyridine-PTyr transformed to a flexible separated random coil structure after blending with P4VP.⁴³

In this present study, we examined the effect of simple noncovalent hydrogen bonding on the structures of supramolecular complexes formed from PTyr and 4-(4-hexadecylphenylazo)pyridine (AzoPy-C16) when using MeOH as a common solvent. We employed Fourier transform infrared (FTIR) spectroscopy, differential scanning calorimetry (DSC), thermogravimetric analysis (TGA), polarized light microscopy (POM), UV-Vis spectroscopy, circular dichroism (CD) spectroscopy, water contact angle (WCA) measurements, small angle X-ray scattering (SAXS), and WAXD to examine the influence of hydrogen bonding on the hierarchical self-assembly and secondary structures of the PTyr/AzoPy-C16 supramolecular complexes.

Experimental section

Materials

4-Aminopyridine, 1-propargylamine, 1-bromohexadecane, MeOH, ethyl acetate (EtOAc), diethyl ether, anhydrous DMF, dichloromethane (DCM), tetrahydrofuran (THF), and hydrochloric acid (HCl, *ca.* 37%) were purchased from Alfa-Aesar. Phenol, anhydrous potassium carbonate (K_2CO_3), anhydrous magnesium sulfate ($MgSO_4$), potassium iodide (KI), sodium hydroxide (NaOH), and sodium nitrite ($NaNO_2$) were obtained from Sigma-Aldrich. L-Tyrosine was purchased from MP Biomedicals. Triphosgene was purchased from TCI. Hexane and acetonitrile (MeCN, 99.5%) were purchased from Acros.

4-(4-Hydroxyphenylazo)pyridine (AzoPy-OH)

Under a N_2 atmosphere, 4-aminopyridine (6.0 g, 64 mmol) was dissolved in 37% HCl (25 mL) in a 250 mL two-neck round-bottom flask while stirring for 20 min below 0 °C (ice bath). A solution of phenol (5.0 g, 58 mmol) and $NaNO_2$ (4.0 g, 58 mmol) in 10% (w/w) aqueous NaOH (45 mL) was added dropwise over 2 h to the flask while maintaining the temperature below 0 °C. The pH of the mixture was adjusted to 6–7 through the addition of 10 wt% aqueous NaOH, affording an orange precipitate. The crude product was collected, washed several times with water, and recrystallized (MeOH/acetone) to give a bright-yellow solid: 3.50 g (60.5%); mp: 263–265 °C (DSC). 1H NMR (δ , DMSO- d_6 , ppm): 10.58 (s, 1H_e), 8.75 (2H, d, ArH_a), 7.89 (2H, d, ArH_b), 7.64 (2H, d, ArH_c), 6.99 ppm (2H, d, ArH_d). ^{13}C NMR (δ , DMSO- d_6 , ppm): 163.37, 157.79, 152.22, 145.89, 126.22, 116.95 ppm. FTIR (KBr, cm^{-1}): 3438 (OH), 1473 (N=N).

4-(4-Hexadecylphenylazo)pyridine (AzoPy-C16) (Scheme 1)

A mixture of 4-(4-hydroxyphenylazo)pyridine (3.0 g, 50 mmol), K_2CO_3 (4.0 g, 100 mmol), and KI (0.10 g, 10 mmol) in DMF (60 mL) was heated in an oil bath at 80 °C for 2 h under a N_2 atmosphere in a 250 mL two neck round-bottom flask equipped with a stirrer bar. 1-Bromohexadecane (7.5 g, 75 mmol) was added dropwise and then the mixture was heated at 80 °C for 24 h. The reaction mixture was extracted with EtOAc (3 \times 60 mL) and dried ($MgSO_4$). The combined extracts were concentrated using a rotary evaporator to give a red solid, which was purified through recrystallization (EtOH) and further purified through column chromatography (SiO_2 ; hexane/EtOAc) to afford an orange powder: 2.00 g (65.6%); mp: 77 °C (DSC). 1H NMR (δ , $CDCl_3$, ppm): 8.75 (2H, d, ArH_a), 7.93 (2H, d, ArH_b), 7.68 (2H, d, ArH_c), 7.03 (2H, d, ArH_d), 4.05 (2H, t, OCH_2), 1.82 (2H, m, OCH_2CH_2), 1.65 (2H, m, CH_2), 1.23 (24H, m, $C_{12}H_{24}$), 0.89 (3H, t, CH_3). ^{13}C NMR (δ , $CDCl_3$, ppm): 163.72, 158.15, 151.87, 147.39, 126.22, 116.55, 69.04, 32.28, 29.68, 25.99, 22.62, 14.09. FTIR (KBr, cm^{-1}): 2848 (aliphatic C–H), 1461 (*trans* N=N).

L-Tyrosine N-carboxyanhydride (Tyr-NCA)⁴²

Triphosgene (2.65 g, 8.85 mmol) was added slowly to a solution of L-tyrosine (4.00 g, 22.10 mmol) in MeCN (150 mL) under reflux (60 °C) for 3 h under a N_2 atmosphere in a 200 mL two-neck round-

bottom flask equipped with a stirrer bar. The resulting solution was cooled to 0 °C in an ice bath and then concentrated through rotary evaporation. The crude product was recrystallized three times from THF/hexane. Yield: 2.80 g (70.0%). ¹H NMR (δ , DMSO-*d*₆, ppm): 9.33 (s, 1H, NH), 9.02 (s, 1H, OH), 6.95 (d, 1H, ArH), 6.69 (d, 2H, ArH), 4.69 (t, 1H, NHCHCH₂), and 2.9 ppm (d, 2H, NHCHCH₂) [Fig. S1(a)†]. ¹³C NMR (δ , DMSO-*d*₆, ppm): 172 (C=O), 157.40 (C=O), 153, 131.44, 125.12, 116, 59, 35.62 [Fig. S2(a)†]. FTIR (KBr, cm⁻¹): 3313 (N-H); 1848 (C=O); 1762 (C=O); 1601 (OH); 1590, 753, and 698 (aromatic ring) [Fig. S3(a)†].

Polytyrosine (PTyr)⁴²

Tyr-NCA (2.00 g, 9.65 mmol) was weighed in a dry three-neck flask under N₂. Anhydrous DMF (10 mL) was injected and the resulting solution stirred for 15 min in an ice bath. Propargylamine (initiator; 0.125 mL, 48.3 mmol) was added and then the reaction mixture was kept at 0 °C for 72 h. The solvent was evaporated under vacuum distillation at 50 °C. The residue was dissolved in MeOH and precipitated in diethyl ether. Yield: 1.50 g, 56%. ¹H NMR (DMSO-*d*₆, δ , ppm): 9.14 (s, 1H, OH), 7.94 (s, 1H, NH), 6.95 (d, 2H, ArH), 6.69 (d, 2H, ArH), 4.40 (t, 1H, NHCHCH₂), 2.9 (d, 2H, NHCHCH₂) [Fig. S1(b)†]. ¹³C NMR (DMSO-*d*₆, δ , ppm): 171.14, 162 (C=O), 156, 130.30, 126.61, 114, 72, 80.97, 72.02, 54.19, 35.27, 31.18 [Fig. S2(b)†]. FTIR (KBr, cm⁻¹): 3288 (N-H); 1655, 1630, 1545 (amide bonds in polymer backbone); 1848 (C=O); 1601, 753, 698 (aromatic ring) [Fig. S3(b)†].

PTyr/AzoPy-C16(x) supramolecular complexes

PTyr/AzoPy-C16(x) complexes were prepared by dissolving AzoPy-C16 and PTyr in MeOH (good solvent; 10 mL). Each sample was stirred for 24 h to ensure complete solubility and the formation of a homogeneous solution. The MeOH from each sample was then slowly evaporated at room temperature over 24 h. The resulting complexes were dried under vacuum at 30 °C to remove any remaining solvent.

Photoisomerization of AzoPy-C16 and PTyr/AzoPy-C16(1)

A solution of AzoPy-C16 or PTyr/AzoPy-C16(1) in methanol (5 mL) was placed in a quartz tube and irradiated for intervals of time at room temperature using a UVP CL-1000 UV cross-linker (UVP, Cambridge, UK) at 365 nm.

Preparation of PTyr and PTyr/AzoPy-C16(1) supramolecular complex film before and after photoisomerization

A solution of PTyr or PTyr/AzoPy-C16(1) (3 wt%) in methanol was passed through a 0.3 μ m syringe filter and then a portion (1 mL) was spin coated (15 000 rpm, 50 s) onto a glass slide (1000 mm \times 100 mm \times 1 mm). The PTyr and PTyr/AzoPy-C16(1) were dried and examined for their surface properties. Then, the PTyr/AzoPy-C16(1) thin film was irradiated under a UVP CL-1000 UV cross-linker at 365 nm.

Characterization

¹H and ¹³C NMR spectra of samples in CDCl₃ and DMSO-*d*₆ were the solvents and tetramethylsilane (TMS) was the internal

reference were recorded using a Varian Unity INOVA 500 MHz spectrometer. FTIR spectra of AzoPy-OH, AzoPy-C16, Tyr-NCA, PTyr, and films of PTyr/AzoPy-C16(x) supramolecular complexes were measured using a Bruker Tensor 27 FTIR spectrophotometer; 32 scans were collected at a spectral resolution of 4 cm⁻¹ at room temperature. Molecular weights and molecular weight distributions (PDI) of PTyr were measured through gel permeation chromatography (GPC) using a Waters 510 high-performance liquid chromatography (HPLC) system equipped with a 410 differential refractometer and three ultrastayragel columns (100, 500, 103 Å) connected in series; DMF was the eluent (flow rate: 0.4 mL min⁻¹). Mass spectra were recorded using a Bruker Daltonics Autoflex III MALDI-TOF mass spectrometer and the following voltage parameters: 19.06 and 16.61 kV for ion sources; 8.78 kV for lens; 21.08 and 9.73 kV for reflectors. DSC measurements of AzoPy-C16, PTyr, and the PTyr/AzoPy-C16(x) supramolecular complexes were performed using a TA Q-20 system, under N₂ as a purge gas (50 mL min⁻¹), at a heating rate of 20 °C min⁻¹; the sample (*ca.* 3–5 mg) was placed in a sealed aluminum sample pan. The thermal stabilities of the PTyr, AzoPy-C16, and PTyr/AzoPy-C16(x) supramolecular complexes were investigated using a TA Q-50 thermogravimetric analyzer, under N₂ as a purge gas (60 mL min⁻¹), at a heating rate of 20 °C min⁻¹ from 30 to 800 °C. The crystallinity and birefringence of AzoPy-C16 and the PTyr/AzoPy-C16(x) complexes were investigated through POM at room temperature; samples were prepared at a concentration of 3 wt% in MeOH. UV-Vis spectra were recorded using a Shimadzu mini 1240 spectrophotometer; the concentration of AzoPy-C16 and PTyr/AzoPy-C16(1) in THF was 10⁻⁴ M. CD spectra were recorded using a JASCO J-810 spectrometer; solutions of the samples were prepared at a concentration of 1 mg mL⁻¹ in MeOH. WAXD profiles were measured using the wiggler beamline BL17A1 of the National Synchrotron Radiation Research Center (NSRRC) of Taiwan; a triangular bent Si (111) single crystal was used to obtain a monochromated beam with a wavelength (λ) of 1.33 Å; samples were annealed prior to WAXD measurement. SAXS experiments were performed using the SWAXS instrument at the BL17B3 beamline of the NSRRC, Taiwan; the X-ray beam had a diameter of 0.5 mm and a wavelength (λ) of 1.24 Å; blend samples (thickness: 1 mm) were sealed between two thin Kapton windows (thickness: 80 μ m) and analyzed at room temperature. WCAs of PTyr and PTyr/AzoPy-C16(x) supramolecular complexes were measured using an FDSA Magic Droplet 100 contact angle goniometer interfaced with image capture software and droplets (5 μ L) of deionized water at room temperature, before and after photoisomerization of the azobenzene units.

Results and discussion

Synthesis of AzoPy-OH and AzoPy-C16

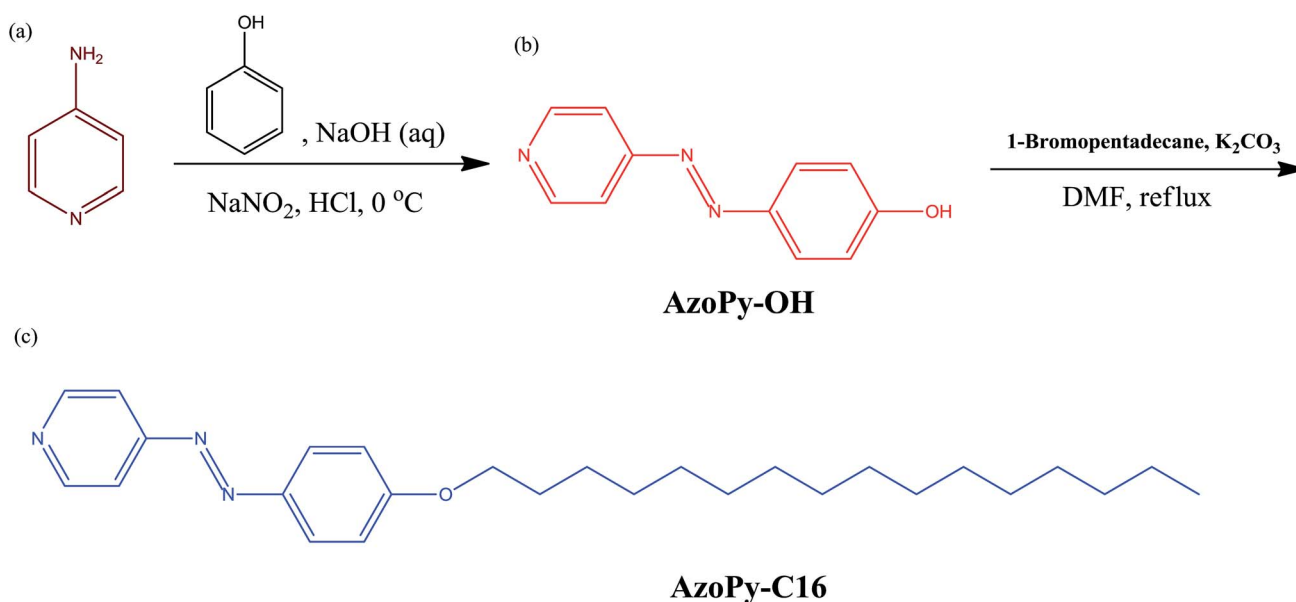
We synthesized 4-(4-hydroxyphenylazo)pyridine (AzoPy-OH) in high yield and high purity through a simple diazonium reaction of 4-aminopyridine with phenol in the presence of HCl, NaNO₂, and NaOH (10 wt%, enough to neutralize the pH of the reaction mixture to 6–7).^{31,44} We then prepared 4-(4-hexadecylphenylazo)pyridine (AzoPy-C16) through monoetherification of AzoPy-OH

with 1-bromohexadecane in the presence of K_2CO_3 and catalytic KI in DMF (Scheme 1).⁴⁵ The molecular structures of AzoPy-OH and AzoPy-C16 were confirmed using 1H and ^{13}C NMR and FTIR spectroscopy. Fig. 1(a) and (b) display the 1H NMR spectra of AzoPy-OH in $DMSO-d_6$ and AzoPy-C16 in $CDCl_3$, respectively. The signal of AzoPy-OH centered at 10.58 ppm corresponds to the proton of the phenolic OH group; those at 8.75–6.99 ppm represent the aromatic protons of the azobenzene pyridine unit.³¹ The 1H NMR spectrum of AzoPy-C16 features characteristic signals at 8.75–7.03 ppm for the aromatic protons of the azobenzene pyridine unit; at 4.05, 1.82, and 1.23 ppm for the methylene protons of the OCH_2CH_2 , OCH_2CH_2 , and $C_{12}H_{24}$ groups, respectively; and at 0.89 ppm for the methyl group (CH_2CH_3). The absence of the signal for the OH group of AzoPy-OH at 10.58 ppm confirmed the successful synthesis of AzoPy-C16. Fig. 1(c) and (d) present the ^{13}C NMR spectra of AzoPy-OH and AzoPy-C16, respectively. The chemical shifts of the aromatic carbon nuclei of the azobenzene pyridine moiety appear in the range from 163.37 to 116.95 ppm. New signals were clearly evident at 69.04, 32.28, 25.99, 22.62, and 14.09 ppm in the spectrum of AzoPy-C16, assignable to the carbon nuclei of the OCH_2 , OCH_2CH_2 , $CH_2CH_2CH_2$, $CH_2CH_2CH_3$, and CH_3 groups, respectively. In the FTIR spectrum of AzoPy-OH [Fig. 1(e)], characteristic absorption signals appear at 3438 (stretching of the phenolic OH group), 3040 (stretching of aromatic CH bonds), 1440 (*trans* azo group), and 1600 and 1576 ($C=C$ stretching of aromatic ring in azobenzene pyridine ring) cm^{-1} . The FTIR spectrum of AzoPy-C16 features absorption bands at 3034 cm^{-1} for stretching of the aromatic CH bonds and at 2920 cm^{-1} for stretching of the aliphatic CH bonds; as expected, it does not contain a signal for a phenolic OH group. The DSC trace in Fig. 1(g) reveals that AzoPy-C16 is a crystalline compound with a sharp melting peak at 77 °C. Taken together, these analyses confirmed the successful syntheses of AzoPy-OH and AzoPy-C16.

We synthesized Tyr-NCA and PTyr according to previous reports; 1H and ^{13}C NMR and FTIR spectroscopy confirmed their chemical structures (Fig. S1–S3†).^{42,43,46} The number-average (M_n) and weight-average (M_w) molecular weights and polydispersity index (PDI) of our sample of PTyr were 2570 $g\ mol^{-1}$, 3100 $g\ mol^{-1}$, and 1.20, respectively, as determined through MALDI-TOF (Fig. 2) and GPC (Fig. S4†) analysis.

Thermal properties of PTyr/AzoPy-C16(x) supramolecular complexes

We prepared the supramolecular complexes PTyr/AzoPy-C16(x) (where x is the number of azopyridine units per PTyr repeating unit) by mixing a desired amount of a PTyr solution with corresponding molar ratios of AzoPy-C16 in MeOH and then evaporating the solvent at room temperature. To investigate the influence of AzoPy-C16 on the thermal stability, we examined the secondary structure of the polypeptide, the optical properties, and the surface features of the PTyr/AzoPy-C16(x) supramolecular complexes using a combination of DSC, TGA, FTIR spectroscopy, UV-Vis absorption spectroscopy, POM, WAXD, SAXS, and WCA measurements. Fig. 3 displays the results of DSC analysis of the thermal behavior of PTyr/AzoPy-C16(x) supramolecular complexes in solid state. Pure AzoPy-C16 was a crystalline compound with sharp melting and crystallization peaks at 77 and 63 °C (Fig. S5†), respectively; pure PTyr was an amorphous polypeptide with a glass transition temperature (T_g) of 151 °C.⁴² Interestingly, the melting and crystallization temperatures of pure AzoPy-C16 increase to 82 and 66 °C, respectively, after blending with the rigid structure of PTyr, as revealed in Fig. 3 and S5.† This result suggested that the packing and crystallization efficiency of the long alkyl chains of AzoPy-C16 increased as a result of confinement of AzoPy-C16 by the PTyr homopolymer.⁴⁸ The values of T_g of polymers often decrease after hydrogen bonding with azobenzene moieties, attributable to the plasticization effect



Scheme 1 (a) Aminopyridine, synthesis of (b) AzoPy-OH and (c) AzoPy-C16 through the diazonium and etherification reactions.

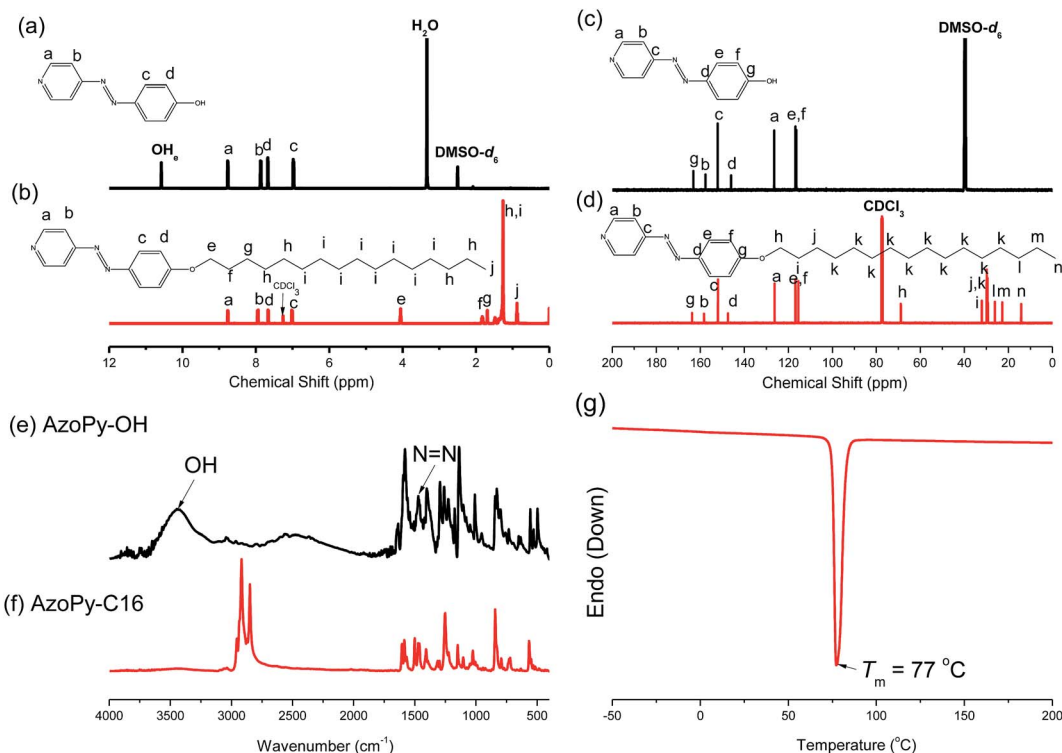


Fig. 1 (a and b) ^1H and (c and d) ^{13}C NMR spectra of (a and c) AzoPy-OH in $\text{DMSO}-d_6$ and (b and d) AzoPy-C16 in CDCl_3 . (e and f) FTIR spectra of (e) AzoPy-OH and (f) AzoPy-C16, recorded at room temperature. (g) DSC analysis of AzoPy-C16 (first run heating scan).

of the azobenzene units.⁴⁷ As revealed in Fig. 3, however, the glass transition temperatures of our supramolecular complexes PTyr/AzoPy-C16 (162 °C) were higher than that of pure PTyr (151 °C) when we increased the value of x from 0 to 4, presumably because of hydrogen bonding between the pyridine units in the AzoPy-C16 moieties and the OH groups in PTyr.⁴² To further investigate the influence of hydrogen bonding on the thermal stability of PTyr, we performed TGA analyses of AzoPy-C16 and the supramolecular complexes PTyr/AzoPy-C16(x) (Fig. 4). The degradation temperatures T_{d5} and T_{d10} and the char yield of pure AzoPy-C16 were 275

and 293 °C and 2%, respectively; for PTyr, these values were 123 and 180 °C and 28%, respectively. The char yields of PTyr/AzoPy-C16(0.25) and PTyr/AzoPy-C16(0.7) were 25 and 19%, respectively. These results confirmed that hydrogen bonding between the pyridine units of the AzoPy-C16 moieties and the OH groups of PTyr enhanced the thermal stability of AzoPy-C16. Table S1† summarizes the TGA data for PTyr, AzoPy-C16, and the PTyr/AzoPy-C16(x) complexes. We also used POM to study the birefringence and crystallinity of AzoPy-C16 and the PTyr/AzoPy-C16(1) supramolecular complex at room temperature (Fig. 5). The images revealed the birefringence and maintained crystallinity of the AzoPy-C16 moieties within the PTyr homopolymer.

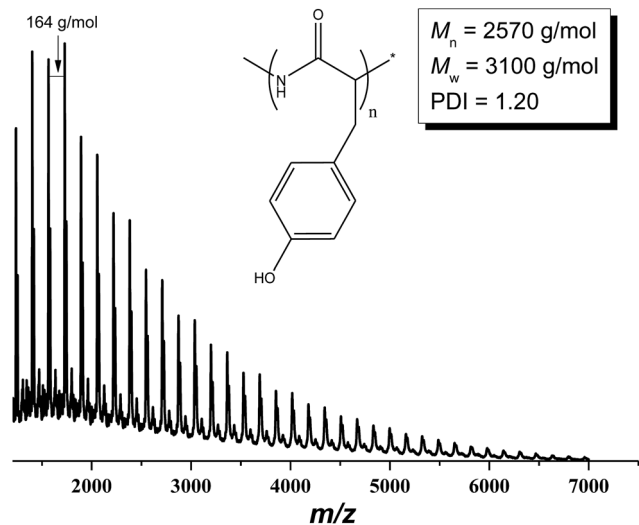


Fig. 2 MALDI-TOF mass spectrum of PTyr.

Secondary and self-assembled structures of PTyr/AzoPy-C16(x) supramolecular complexes

We used FTIR spectroscopy to examine the specific interactions between the pyridine units in the AzoPy-C16 moieties and the OH groups of PTyr, as well as the secondary structure of the polypeptide formed as a result of these hydrogen bonding interactions.^{49,50} Fig. S6† displays FTIR spectra of PTyr, AzoPy-C16, and the PTyr/AzoPy-C16(x) supramolecular complexes, recorded at room temperature and presented in the range 1030–970 cm^{-1} . The characteristic stretching vibrations of AzoPy-C16 are centered at 1590, 1050, 993, and 625 cm^{-1} , all of which can be assigned to its free pyridyl unit. Pure PTyr provided a characteristic band at 1015 cm^{-1} . Here, we used the characteristic band of AzoPy-C16 at 993 cm^{-1} to investigate the degree of hydrogen bonding between the pyridyl group and the OH groups of PTyr. The intensity of the absorption band at 993 cm^{-1} of the free pyridyl moiety of AzoPy-

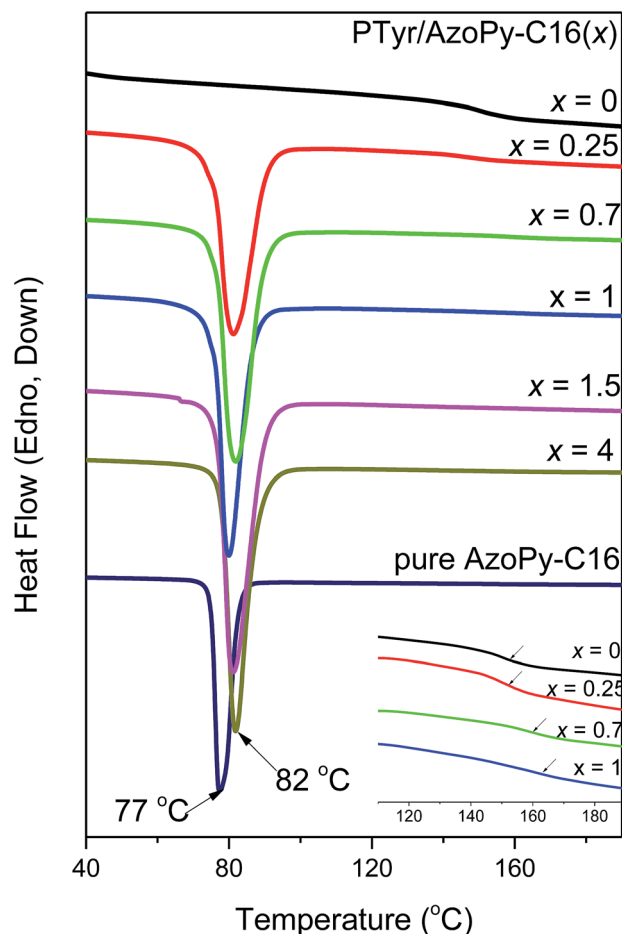


Fig. 3 DSC profiles of PTyr, AzoPy-C16, and PTyr/AzoPy-C16(x) supramolecular complexes.

C16 decreased slightly and shifted after forming the PTyr/AzoPy-C16(x) complexes, with a new signal appearing at 1010–1015 cm^{-1} that represented the hydrogen-bonded pyridine ring of AzoPy-C16 interacting with the OH groups of PTyr. Although this new absorption band at 1010–1015 cm^{-1} overlapped with the original stretching vibration signal of AzoPy-C16, the

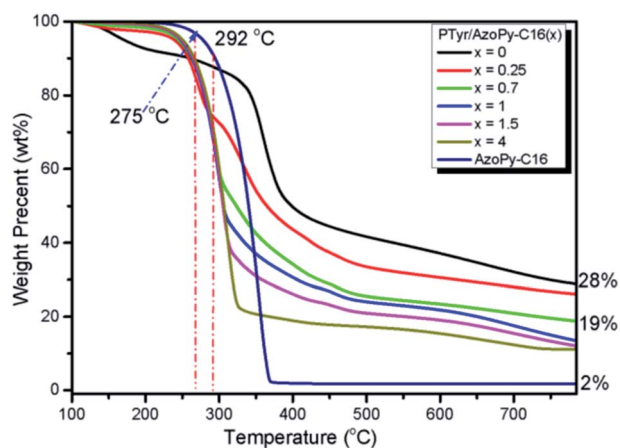


Fig. 4 TGA analyses of PTyr, AzoPy-C16, and PTyr/AzoPy-C16(x) supramolecular complexes, recorded under N_2 atmospheres.

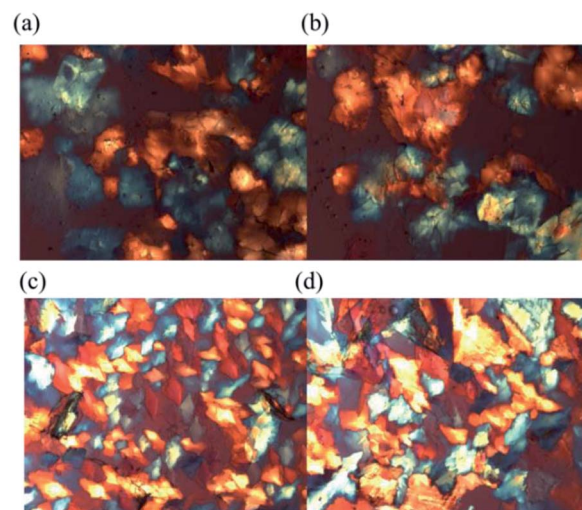


Fig. 5 POM images of (a and b) AzoPy-C16 and (c and d) the PTyr/AzoPy-C16(1) supramolecular complex, recorded at room temperature.

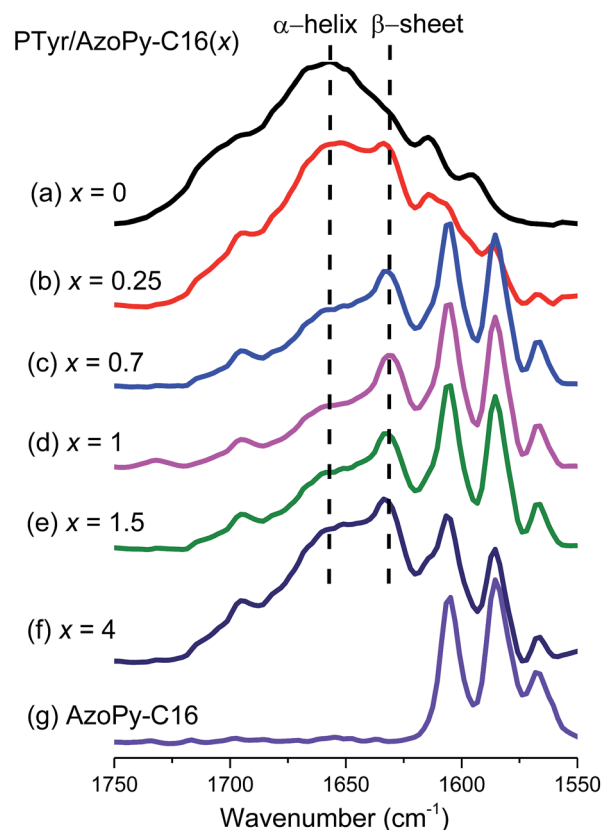


Fig. 6 FTIR spectra (1750–1580 cm^{-1}) of PTyr/AzoPy-C16(x) supramolecular complexes, recorded at room temperature.

combination of DSC, TGA, and FTIR spectroscopic analyses were consistent with supramolecular interactions between PTyr and AzoPy-C16 being hydrogen bonds.

Our main goal in this study was to investigate the influence of AzoPy-C16 on the secondary structure of the polypeptide. Many polypeptides form well-defined secondary structures (α -

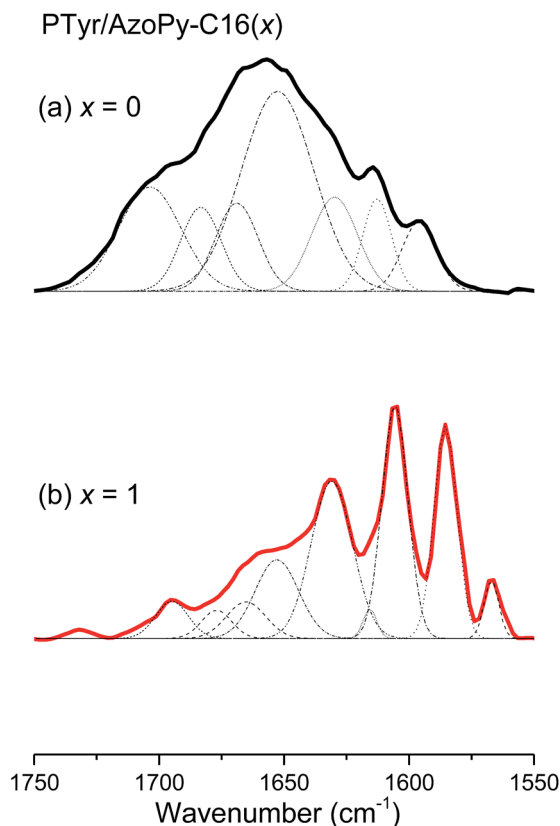


Fig. 7 An example of curve fitting of the results in Fig. 6 for PTyr/AzoPy-C16(x) supramolecular complexes.

helices, β -sheets) as well as random coils. Fig. 6 displays FTIR spectra of PTyr, AzoPy-C16, and PTyr/AzoPy-C16(x) complexes, recorded at room temperature and presented in the range 1750–1580 cm^{-1} , that we used to deduce the secondary structure of PTyr in the supramolecular complexes. The spectrum of PTyr features signals at 1597 and 1615 cm^{-1} corresponding to stretching absorptions of the tyrosine ring; at 1655 cm^{-1} for an α -helical conformation; at 1630 cm^{-1} for a β -sheet conformation; at 1670 cm^{-1} for a β -turn conformation; and at 1643, 1683, and 1700 cm^{-1} for a random-coil conformation.^{42,43,51,52} We used curve fitting (Fig. 7) to determine the fractions of each secondary structure; Fig. 8 summarizes in the results. The fraction of PTyr structures with α -helical conformations decreased and those with β -sheet conformations increased upon increasing the value of x in the PTyr/AzoPy-C16(x) complexes from 0.25 to 1 (*i.e.*, the degree of complexation of the pyridine units with the OH groups of PTyr). Jeon *et al.* reported that the mobility of the side chain groups of polypeptides strongly affects their secondary structures; they found experimentally that flexible alkyl side chains induce weaker intramolecular hydrogen bonds for amide linkages in α -helical conformations, thereby decreasing the fraction of α -helical conformations.⁵⁴ Our present results are consistent with theirs: the long alkyl chains of the AzoPy-C16 moieties presumably weakened the hydrogen bonds between the C=O and NH units of PTyr in the α -helical conformations, such that the fraction of α -helical conformations decreased upon increasing the concentration of AzoPy-C16. The fractions of α -helical and β -sheet conformations of pure PTyr were 44.7 and 13.3%,

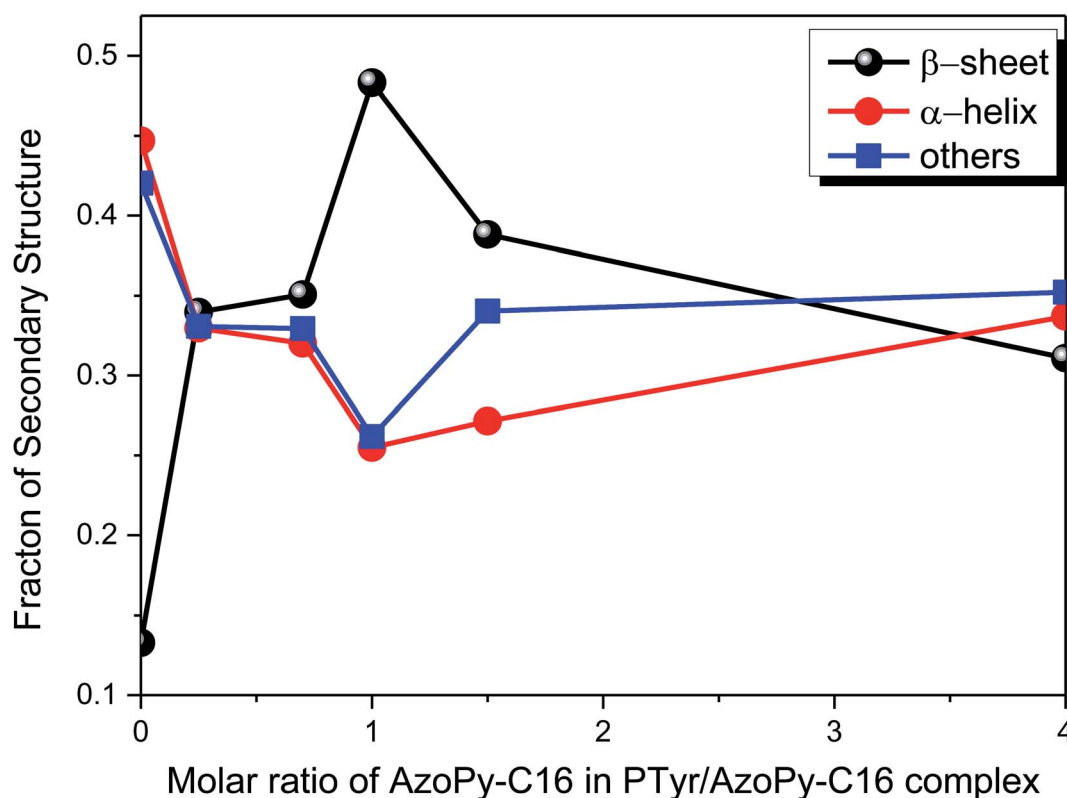


Fig. 8 Fractions of secondary structures in PTyr/AzoPy-C16 supramolecular complexes at various AzoPy-C16 concentrations.

respectively, whereas the PTyr/AzoPy-C16(1) supramolecular complex featured the lowest fraction of α -helical conformations and the highest fraction of β -sheet conformations—25.5 and 48.3%, respectively—with its equal molar ratio of pyridine moieties and phenolic OH groups. Further increasing the concentration of AzoPy-C16 to excess, the fraction of α -helical conformations increased and the fraction of β -sheet conformations decreased, as expected. Thus, the fractions of secondary structural conformations of PTyr were strongly dependent on the intermolecular interactions in the PTyr/AzoPy-C16 supramolecular complexes.

CD is a convenient method for determining the secondary structures of polypeptides in solution.^{54,55} α -Helical conformations in a CD profile are characterized by two negative bands at 208 and 222 nm and a strong positive band at 192 nm; β -sheet structures (well-defined antiparallel β -pleated sheets) have a negative minimum band at 218 nm and a positive maximum band at 198 nm; a small positive band at 218 nm and a negative band near to 200 nm appear for randomly coiled polypeptides.^{56–60} We recorded CD spectra to examine the secondary structures of pure PTyr and the PTyr/AzoPy-C16(0.25) and PTyr/AzoPy-C16(1) supramolecular complexes in MeOH solution at a concentration of 10^{-4} M (Fig. 9). Although Ishii *et al.* reported^{61c} that basic CD spectroscopy itself might not be useful for identifying the conformations of PTyr, because it mainly reflects the optical rotation from the La transitions of the phenolic rings on the PTyr side chain, they employed fluorescence detected circular dichroism (FD-CD) spectroscopy to examine the secondary structures of PTyr. In MeOH solution, the backbone of PTyr was represented by two negative bands at 213 and 222 nm, which were attributed to α -helical conformations; when an aqueous solution of NaOH was added to the MeOH solution of PTyr, the structure of PTyr transformed from an α -helical to a β -sheet conformation.⁶¹ Fig. 9 reveals that pure PTyr provided a strong positive band at 242 nm and a negative band at 203 nm. After blending with AzoPy-C16 at values of x of 0.25 and 1.0, the positive band at 242 nm and a negative band at 203 nm were decreased and disappeared, respectively. A new positive band at

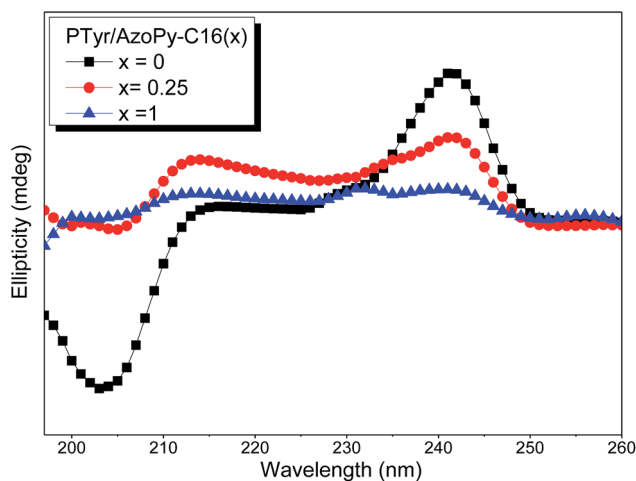


Fig. 9 CD spectra of PTyr, PTyr/AzoPy-C16(0.25), and PTyr/AzoPy-C16(1) in MeOH (2.0 mg mL^{-1}).

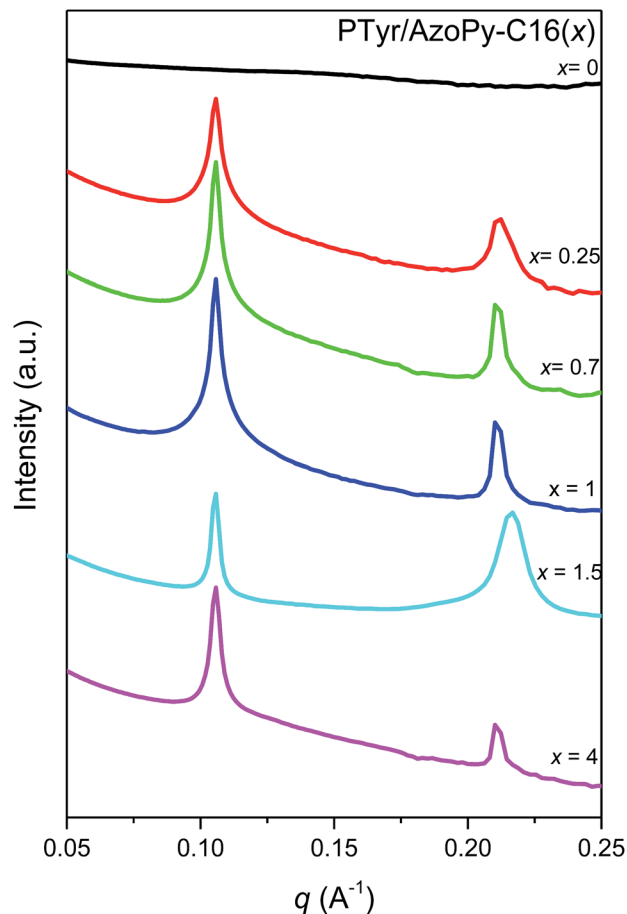
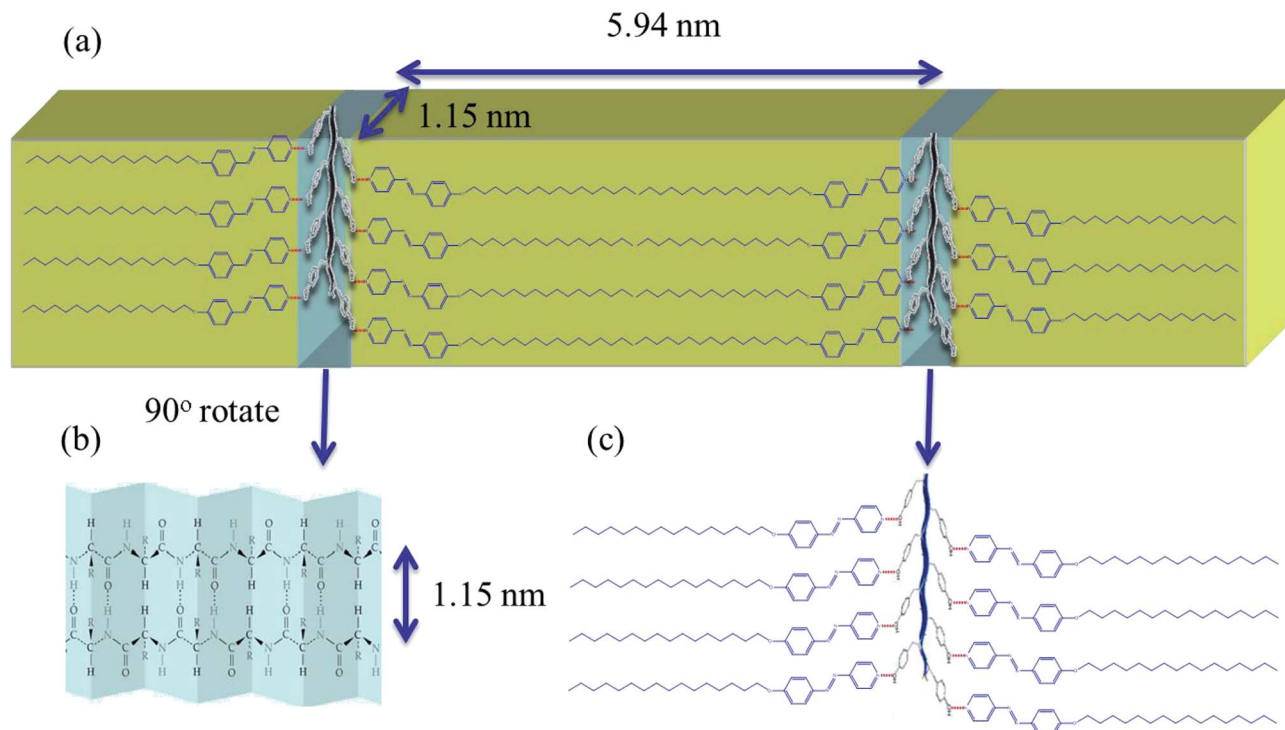


Fig. 10 SAXS curves of PTyr, AzoPy-C16, and PTyr/AzoPy-C16(x) complexes, recorded at room temperature.

213 nm appeared, suggesting to transformation from the α -helical conformation of PTyr to the β -sheet structure, consistent with the FTIR spectroscopic data.

Next, we investigated the self-assembled structures formed by the PTyr/AzoPy-C16(x) supramolecular complexes in the bulk state after annealing at 200°C and then slowly cooling to room temperature. Fig. 10 displays SAXS profiles of the resulting PTyr/AzoPy-C16(x) supramolecular complexes. Two sharp diffraction peaks appeared at 0.1055 ($d = 5.94 \text{ nm}$) and 0.211 ($d = 2.97 \text{ nm}$) when the value of x was increased from 0.25 to 4. The ratio of the diffraction scattering vectors (q/q_m) of these two sharp peaks was $1 : 2$, indicating a long-range-ordered lamellar structure of AzoPy-C16 within PTyr with a perfect d -spacing of 5.94 nm , as depicted in Scheme 2.

We also used WAXD to examine the changes in the secondary conformations and the crystallinity of the PTyr/AzoPy-C16 supramolecular complexes. Fig. 11 presents WAXD profiles of pure PTyr, pure AzoPy-C16, and the PTyr/AzoPy-C16(x) supramolecular complexes, all recorded at room temperature. The profile of PTyr features many diffraction peaks. For example, a diffraction scattering peak located at a value of q of 0.54 \AA^{-1} (1.15 nm), corresponding to the distance between the backbones in the antiparallel β -pleated sheet structure. Higher-order diffraction peaks appeared with values of q/q_m of 1, 2, 3, and 4,



Scheme 2 Cartoon representations of (a) the possible hierarchical lamellae-within-lamellae structure, (b) the distance between the backbones in the antiparallel β -pleated sheet structure, and (c) the intermolecular hydrogen bonding within PTyr/AzoPy-C16 supramolecular complexes.

implying that pure PTyr possessed a long-range-ordered lamellar structure. In addition, the signal at a value of q of 1.32 \AA^{-1} ($d = 0.475 \text{ nm}$) mainly corresponded to the intermolecular distance between adjacent peptide chains within the lamellar structure. Meanwhile, the diffraction peak at 1.45 \AA^{-1} ($d = 0.445 \text{ nm}$) was due to the repeated residues of the peptide chain.^{42,43} The WAXD profile of pure AzoPy-C16 also featured many ordered and sharp peaks, consistent with it being a crystalline compound. The long-range order of a lamellar structure was revealed by peak ratios of 2 : 3 : 4 : 5 : 6 for pure AzoPy-C16, consistent with the SAXS results. In addition, two diffraction peaks appeared for pure AzoPy-C16 at 1.49 \AA^{-1} ($d = 0.42 \text{ nm}$) and 1.70 \AA^{-1} ($d = 0.37 \text{ nm}$), corresponding to crystallization of the long aliphatic tails of AzoPy-C16 moieties in an orthorhombic structure.⁶² Interestingly, when the value of x increased from 0.25 to 4 for the PTyr/AzoPy-C16(x) supramolecular complexes, the sharp diffraction scattering peaks of AzoPy-C16 remained dominant, presumably because the azobenzene derivative with the long alkyl carbon chain (C16) wrapped around the PTyr backbone and formed hydrogen bonds between its pyridyl group and the OH groups of PTyr, thereby increasing the crystallinity of AzoPy-C16 when sequestered within the lamellar structure.⁶³ As a result, we propose a hierarchical lamellae-within-lamellae architecture for the complexes, featuring a long-range-ordered lamellar structure from the alkyl groups of AzoPy-C16 ($d = 5.94 \text{ nm}$) and a long-range-ordered lamellar structure from the antiparallel β -pleated sheet conformation of PTyr ($d = 1.15 \text{ nm}$), oriented perpendicularly, as displayed in Scheme 2.

We investigated the effect of temperature on the conformational changes and behavior of the β -sheet secondary structure in

the supramolecular complexes by recording variable-temperature FTIR spectra of PTyr/AzoPy-C16(0.25) and PTyr/AzoPy-C16(1.5) at temperatures from 25 to 150 °C [Fig. 12(a) and (b), respectively]. We observed no obvious changes to the β -sheet conformation upon increasing the temperature, indicating that the β -sheet secondary structure was quite stable to the conditions.^{14,53} This result was confirmed in the WAXD analyses of the PTyr/AzoPy-C16(0.25) and PTyr/AzoPy-C16(1.5) supramolecular complexes performed at various temperatures (Fig. 13). As expected, the long-period peaks of the lamellar structure and the crystalline peaks from the orthorhombic structure disappeared when the temperature was higher (>90 °C) than the melting temperature (*ca.* 80 °C) of AzoPy-C16. The β -sheet conformation, represented by signals at values of q of 0.54, 1.32, and 1.45 \AA^{-1} , was maintained, however, upon increasing the temperature, indicating high stability for this structure under these conditions.

Photoresponsive behavior of PTyr/AzoPy-C16(x) supramolecular complexes

We recorded UV-Vis spectra to examine the photoisomerization of the azobenzene units in MeOH solutions of pure AzoPy-C16 and PTyr/AzoPy-C16(1) after various periods of time under irradiation with UV light (365 nm), as presented in Fig. 14(a) and (b), respectively. The absorption peaks of AzoPy-C16 and the supramolecular complex appeared initially at 353 nm and 442 nm, corresponding to π - π^* and n - π^* transitions of the *trans* isomers. After the solutions of AzoPy-C16 and PTyr/AzoPy-C16(1) had been exposed to the UV light, the absorption peak for the *trans*-azobenzene isomers decreased after 15 min for

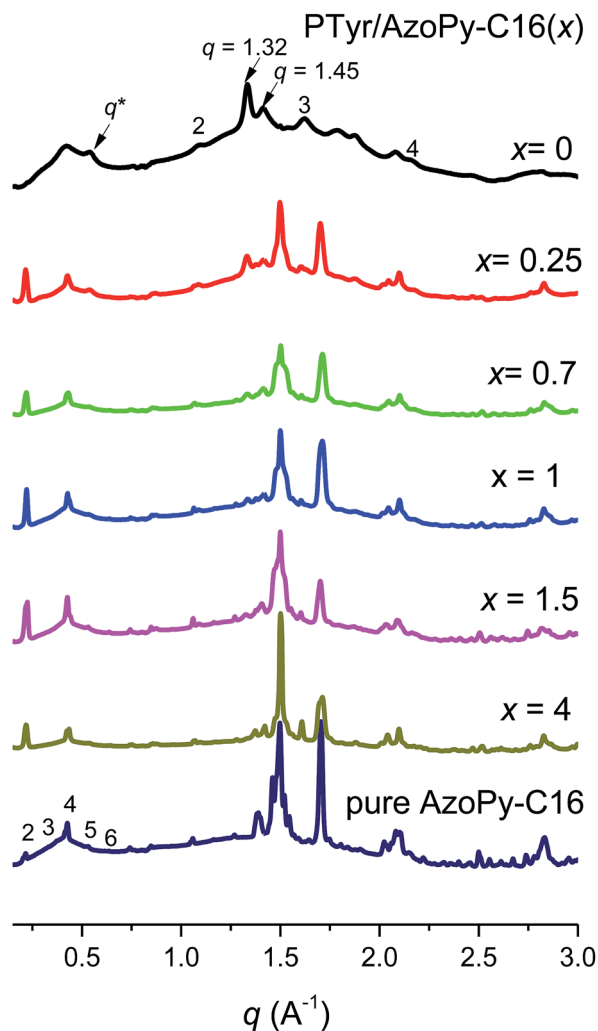


Fig. 11 WAXD analyses of PTyr/AzoPy-C16(*x*) complexes, recorded at room temperature.

AzoPy-C16 and 90 min for PTyr/AzoPy-C16(1), with corresponding increases in the intensity of the absorption signals near 442 nm, corresponding to $n-\pi^*$ transitions of the *cis* isomers. We calculated the degree of photoisomerization of the azobenzene moieties in AzoPy-C16 and PTyr/AzoPy-C16(1) using the equation^{31,44,45}

$$\text{Photoisomerization degree} = (A_0 - A_i)/A_0 \times 100\%$$

where A_0 is the absorbance prior to irradiation with UV light and A_i is the absorbance at the same wavelength measured in the photostationary state. The degree of isomerization of the PTyr/AzoPy-C16(1) supramolecular complex (30%) was lower than that of pure AzoPy-C16 (60%), presumably because intermolecular hydrogen bonding of the pyridyl rings of AzoPy-C16 and the OH groups of PTyr was a hindrance to isomerization. Solutions of AzoPy-C16 and PTyr/AzoPy-C16(1) in methanol were kept in dark for 2 days after UV-irradiation at 365 nm. The absorption peaks of $\pi-\pi^*$ and $n-\pi^*$ transition of their *trans* isomer came back to original state. These results indicating that both of AzoPy-C16 and PTyr/AzoPy-C16(1) exhibited photoresponsivity and photoreversibility of

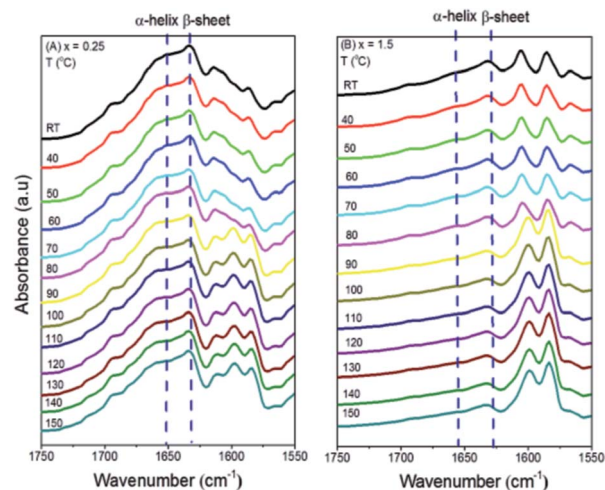


Fig. 12 FTIR spectra of (A) PTyr/AzoPy-C16(0.25) and (B) PTyr/AzoPy-C16(1.5).

azobenzene unit in of AzoPy-C16 and PTyr/AzoPy-C16(1) as presented in Fig. S7(a) and (b).†

Fig. 15 presents the SAXS profiles of the PTyr/AzoPy-C16(1.5) supramolecular complex before and after irradiation with UV light. As mentioned above, PTyr/AzoPy-C16(1.5) provided two sharp diffraction peaks at 0.1055 \AA^{-1} ($d = 5.952 \text{ nm}$) and 0.211 \AA^{-1} ($d = 2.976 \text{ nm}$) prior to UV irradiation. After photoisomerization of PTyr/AzoPy-C16(1.5), the first SAXS peak shifted to a slightly higher value of q , suggesting a decrease in the d -spacing (*ca.* 0.27 nm, 4.5% lower than the original value) consistent with *trans-to-cis* isomerization of the interlayer AzoPy groups. This value is close to the difference in lengths between *trans*-azobenzene (*ca.* 0.9 nm) and *cis*-azobenzene (*ca.* 0.7 nm).⁶⁴ In addition, the conversion of rod-like *trans*-azobenzene to V-shaped *cis*-azobenzene will often induce a decrease in (or loss of) the long-range order of a structure, such as a change from a nematic to an isotropic phase. Therefore, the intensity of the

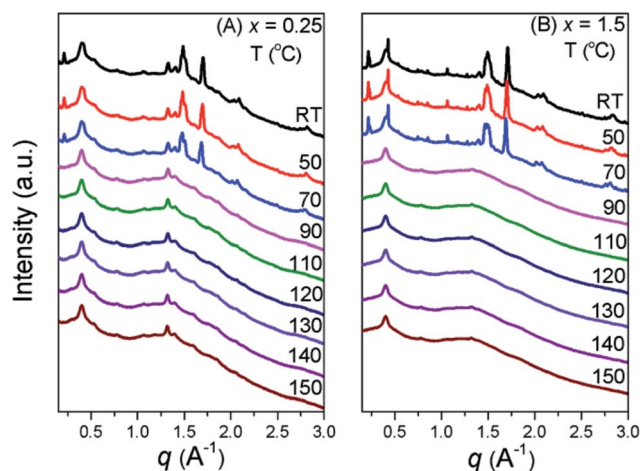


Fig. 13 WAXD profiles of the supramolecular complexes (A) PTyr/AzoPy-C16(0.25) and (B) PTyr/AzoPy-C16(1.5), recorded at temperatures between 25 and 150 °C.

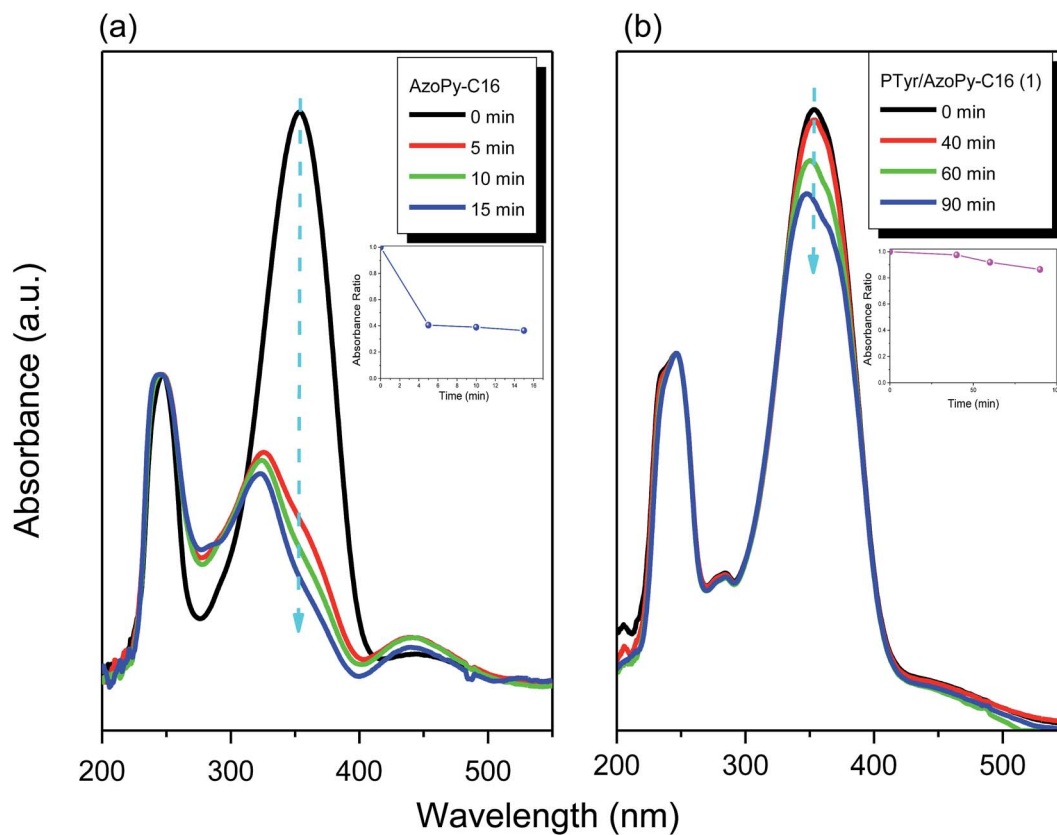


Fig. 14 UV-Vis absorption spectra of (a) AzoPy-C16 and (b) PTyr/AzoPy-C16(1) in MeOH (1×10^{-4} M), recorded after various periods of time under irradiation with UV light.

second scattering peak decreased upon irradiation and eventually disappeared, implying that the long-range order of the lamellar structure of AzoPy-C16 in the supramolecular complex had transformed into a short-range-ordered lamellar structure after photoisomerization.⁶⁵ We observed similar phenomena in the WAXD profiles of the supramolecular complexes PTyr/AzoPy-C16(1) and PTyr/AzoPy-C16(1.5) before and after irradiation with

UV light (Fig. 16). The long-range-ordered lamellar structures, with peak ratios of 2 : 3 : 4 : 5 : 6 : 7, completely disappeared for both of the PTyr/AzoPy-C16(1), and PTyr/AzoPy-C16(1.5) supramolecular complexes after irradiation with UV light. Nevertheless, the orthorhombic structure of the crystallized long aliphatic tails of AzoPy-C16 was not disrupted after irradiation, suggesting

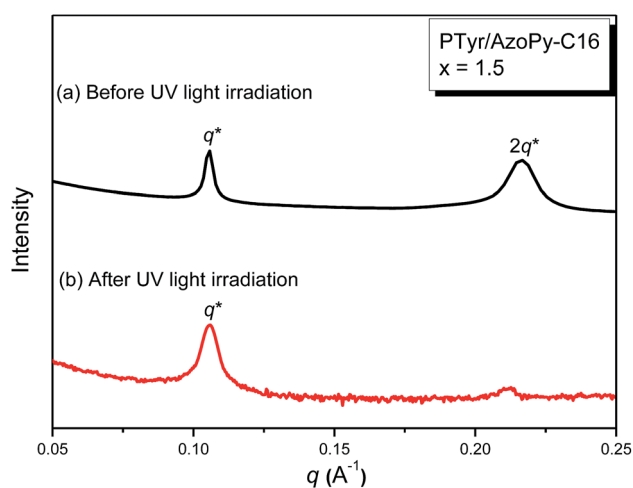


Fig. 15 SAXS profile of the PTyr/AzoPy-C16(1.5) supramolecular complex before and after irradiation with UV light ($\lambda = 365$ nm), recorded at room temperature.

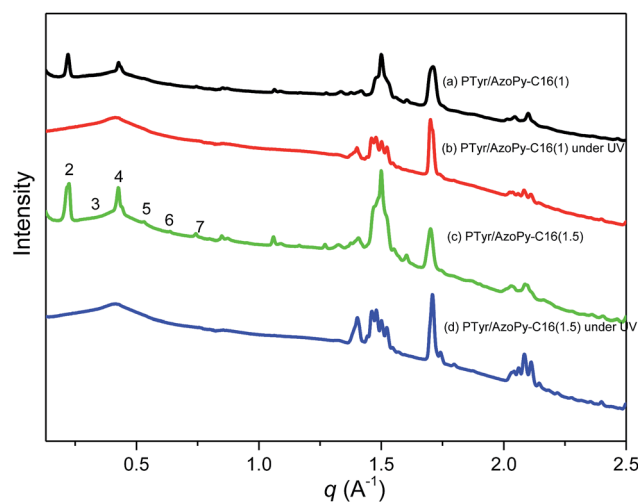


Fig. 16 WAXD profiles of the PTyr/AzoPy-C16(1) and PTyr/AzoPy-C16(1.5) supramolecular complexes before and after irradiation with UV light ($\lambda = 365$ nm), recorded at room temperature.

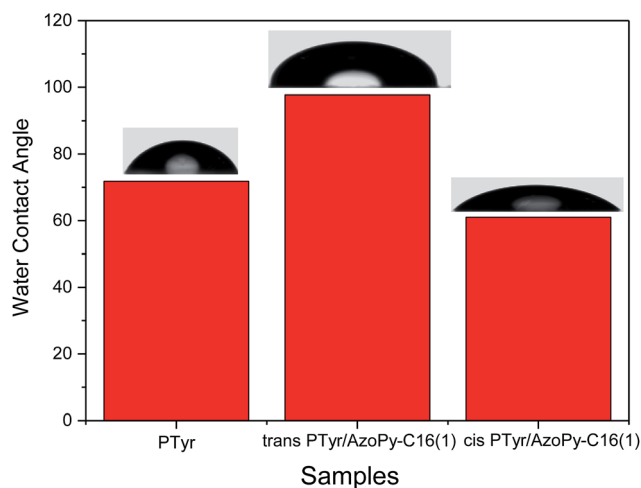


Fig. 17 WCAs of PTyr and the PTyr/AzoPy-C16(1) supramolecular complex before and after photoisomerization under UV light.

that the UV light affected the structure of only the azobenzene group, not the alkyl group, as would be expected.

Next, we examined the hydrophobicity and hydrophilicity of the surfaces of the PTyr/AzoPy-C16 supramolecular complexes before and after irradiation with UV light. Fig. 17 reveals that the WCAs of pure PTyr and the *trans* and *cis* isomers of PTyr/AzoPy-C16(1) were 72.8, 94.2, and 61.3°, respectively. The WCA of the *trans* isomer of PTyr/AzoPy-C16(1) was greater than that of pure PTyr because the long alkyl chains enhanced its hydrophobic properties. After irradiation with UV light, the WCA of the *cis* isomer of PTyr/AzoPy-C16(1) decreased, presumably because (i) the dipole moment of a *cis* isomer is generally higher than that of a *trans* isomer, thereby increasing the surface free energy and leading to a lower WCA, and (ii) photoisomerization of azobenzene molecules typically allows their nitrogen atoms to interact more readily with polar solvents (e.g., water).^{31,66} Therefore, the conformational change from the *trans* form of PTyr/AzoPy-C16 upon irradiation with UV light transformed this hydrophobic supramolecular material into a hydrophilic supramolecular material. We did WCAs measurement to investigate the photoreversibility and photoresponsivity of PTyr/AzoPy-C16(1) supramolecular thin film after UV irradiation at 365 nm for 90 min and kept it in the dark for 2 days at room temperature as shown in Fig. S8.† As shown in Fig. S8,† the wettability of PTyr/AzoPy-C16(1) supramolecular thin film can return to *trans* isomer (more hydrophobic) after leaving in the dark for 2 days through three cycles of measurements.

Conclusions

We have synthesized AzoPy-C16 in high yield and purity. DSC and TGA analyses revealed that the thermal properties of AzoPy-C16 were enhanced after incorporation into the PTyr homopolymer in the form of a comb-like polypeptide supramolecular complex, due to intermolecular hydrogen bonding between the pyridyl groups of AzoPy-C16 and the OH groups of PTyr. FTIR and CD spectroscopy revealed that the secondary structure of

PTyr changed from an α -helical conformation initially to a β -sheet conformation in the complex because the long alkyl chains of the AzoPy-C16 moieties disrupted the hydrogen bonding between the C=O and NH units that stabilized the α -helical conformation of PTyr. Based on SAXS and WAXD analyses, we propose a hierarchical lamellae-within-lamellae structure for the PTyr/AzoPy-C16 supramolecular complexes, with a long-range-ordered lamellar structure from the antiparallel β -pleated sheet conformation of PTyr within, and oriented perpendicularly to, a long-range-ordered lamellar structure arising from the alkyl chains of AzoPy-C16. Furthermore, UV irradiation of the PTyr/AzoPy-C16 supramolecular complex caused the *d*-spacing of the long-range-ordered structure of the alkyl groups to decrease, as did the WCA as a result of the hydrophobic surface transforming into a hydrophilic surface. Our findings suggest that such materials might be good candidates for use in polymer coatings.

Acknowledgements

This work was financially supported by the Ministry of Science and Technology, Taiwan, under contract MOST 102-2221-E-110-008-MY3.

References

- 1 Y. Shen, X. Fu, W. Fu and Z. Li, *Chem. Soc. Rev.*, 2015, **44**, 612–622.
- 2 J. Huang and A. Heise, *Chem. Soc. Rev.*, 2013, **42**, 7373–7390.
- 3 H. Y. Tang, Y. C. Li, S. H. Lahasky, S. S. Sheiko and D. H. Zhang, *Macromolecules*, 2011, **44**, 1491–1499.
- 4 T. J. Deming, *Nat. Mater.*, 2010, **9**, 535–536.
- 5 H. Dong, Y. Y. Shu, N. Dube, Y. F. Ma, M. V. Tirrell, K. H. Downing and T. Xu, *J. Am. Chem. Soc.*, 2012, **134**, 11807–11814.
- 6 J. Zou, F. Zhang, Y. Chen, J. E. Raymond, S. Zhang, J. Fan, J. Zhu, A. Li, K. Seetho, X. He, D. J. Pochan and K. L. Wooley, *Soft Matter*, 2013, **9**, 5951–5958.
- 7 H. R. Kricheldorf, *Angew. Chem., Int. Ed.*, 2006, **45**, 5752–5784.
- 8 J. Fan, R. Li, X. He, K. Seetho, F. Zhang, J. Zou and K. L. Wooley, *Polym. Chem.*, 2014, **5**, 3977–3981.
- 9 H. F. Lee, H. S. Sheu, U. S. Jeng, C. F. Huang and F. C. Chang, *Macromolecules*, 2005, **38**, 6551–6585.
- 10 Y. Shen, S. Desseaux, B. Aden, B. S. Lokitz, S. M. Kilbey, Z. Li and H. A. Klok, *Macromolecules*, 2015, **48**, 2399–2406.
- 11 (a) S. W. Kuo, H. F. Lee, W. J. Huang, K. U. Jeong and F. C. Chang, *Macromolecules*, 2009, **42**, 1619–1626; (b) J. Zou, F. Zhang, Y. Chen, J. E. Raymond, S. Zhang, J. Fan, J. Zhu, A. Li, K. Seetho, X. He, D. J. Pochan and K. L. Wooley, *Soft Matter*, 2013, **9**, 5951–5958.
- 12 P. Papadopoulos, G. Floudas, G. A. Klok, I. Schnell and T. Pakula, *Biomacromolecules*, 2004, **5**, 81–91.
- 13 (a) S. W. Kuo and H. T. Tsai, *Polymer*, 2010, **51**, 5605–5620; (b) A. Top, S. Zhong, C. Yan, C. J. Roberts, D. J. Pochan and K. L. Kiick, *Soft Matter*, 2011, **7**, 9758–9766.

- 14 J. Susanna, H. Sirkku, R. J. Oakley, S. Nummelin, J. Ruokolainen, C. F. J. Faul and O. Ikkala, *Biomacromolecules*, 2009, **10**, 2787–2794.
- 15 A. C. Engler, H. Lee and P. T. Hammond, *Angew. Chem., Int. Ed.*, 2009, **48**, 9334–9338.
- 16 Y. Huang, Y. Zeng, J. Yang, Z. Zeng, F. Zhu and X. Chen, *Chem. Commun.*, 2011, **47**, 7509–7511.
- 17 H. Tang and D. Zhang, *Polym. Chem.*, 2011, **2**, 1542–1551.
- 18 H. Lu and J. Cheng, *J. Am. Chem. Soc.*, 2008, **130**, 12562–12563.
- 19 K. Inomata, Y. Iguchi, K. Mizutani, H. Sugimoto and E. Nakanishi, *ACS Macro Lett.*, 2012, **1**, 807–810.
- 20 K. Inomata, M. Kasuya, H. Sugimoto and E. Nakanishi, *Polymer*, 2005, **46**, 10035–10044.
- 21 C. Deng, J. Wu, R. Cheng, F. Meng, H. A. Klok and Z. Zhong, *Prog. Polym. Sci.*, 2014, **39**, 330–364.
- 22 B. Bucca, K. Horvati, S. Bosze, F. Andreae and C. O. Kappe, *J. Org. Chem.*, 2008, **73**, 7532–7542.
- 23 N. Hadjichristidis, H. Iatrov, M. Pitsikalis and G. Sakellariou, *Chem. Rev.*, 2009, **109**, 5528–5578.
- 24 (a) T. J. Deming, *Adv. Polym. Sci.*, 2006, **202**, 1–18; (b) X. Liao, G. Chen, X. Liu, W. Chen, F. Chen and M. Jiang, *Angew. Chem., Int. Ed.*, 2010, **49**, 4409–4413; (c) J. Zou, B. Guan, X. Liao, M. Jiang and F. Tao, *Macromolecules*, 2009, **42**, 7465–7473.
- 25 J. Li, N. Zhou, Z. Zhang, Y. Xu, X. Chen, Y. Tu, Z. Hu and X. Zhu, *Chem.-Asian J.*, 2013, **8**, 1095–1100.
- 26 Y. Naikane, K. Kitamoto and N. Tamaoki, *Org. Lett.*, 2002, **4**, 3907–3910.
- 27 M. G. Mohamed, C. H. Hsiao, K. C. Hsu, F. L. Lue, H. K. Shih and S. W. Kuo, *RSC Adv.*, 2015, **5**, 12763–12772.
- 28 Y. Chen, H. Yu, L. Zhang, H. Yang and Y. Lu, *Chem. Commun.*, 2014, **50**, 9647–9649.
- 29 T. Seki, S. Nagano and M. Hara, *Polymer*, 2013, **54**, 6053–6066.
- 30 H. F. Yu and T. Ikeda, *Adv. Mater.*, 2011, **23**, 2149–2180.
- 31 H. F. Yu, *Prog. Polym. Sci.*, 2014, **39**, 781–815.
- 32 M. G. Mohamed, W. C. Su, Y. C. Lin, C. F. Wang, J. K. Chen, K. U. Jeong and S. W. Kuo, *RSC Adv.*, 2014, **4**, 50373–50385.
- 33 Y. Chen, M. Quan, H. Yu, L. Zhang, H. Yang and Y. Lu, *RSC Adv.*, 2015, **5**, 31219–31225.
- 34 N. Kawatsuki, H. Miki, M. Kondo and M. Nakamura, *Langmuir*, 2012, **28**, 4534–4542.
- 35 H. Yu, H. Liu and T. Kobayashi, *ACS Appl. Mater. Interfaces*, 2011, **3**, 1333–1340.
- 36 T. F. A. de Greef, M. M. J. Smulders, M. Wolffs, A. P. H. J. Schenning, R. P. Sijbesma and E. W. Meijer, *Chem. Rev.*, 2009, **109**, 5687–5754.
- 37 C. Kulkarni, S. Balasubramanian and S. J. George, *ChemPhysChem*, 2013, **14**, 661–673.
- 38 J. W. Wackerly and J. S. Moore, *Macromolecules*, 2006, **39**, 7164–7276.
- 39 M. T. Stone and J. S. Moore, *J. Am. Chem. Soc.*, 2005, **127**, 5928–5935.
- 40 C. Rest, R. Kandanli and G. Fernández, *Chem. Soc. Rev.*, 2015, **44**, 2543–2572.
- 41 S. W. Kuo and C. J. Chen, *Macromolecules*, 2011, **44**, 7315–7326.
- 42 (a) S. W. Kuo and C. J. Chen, *Macromolecules*, 2012, **45**, 2442–2452; (b) S. Wu, J. Huang, S. Beckemper, A. Gillner, K. Wang and C. Bubeck, *J. Mater. Chem.*, 2012, **22**, 4989; (c) A. Priimagi, J. Vapaavuori, F. J. Rodriguez, C. F. J. Faul, M. T. Heino, O. Ikkala, M. Kauranen and M. Kaivola, *Chem. Mater.*, 2008, **20**, 6358–6363; (d) J. E. Koskela, J. Vapaavuori, R. H. A. Ras and A. Priimagi, *ACS Macro Lett.*, 2014, **3**, 1196–1200; (e) S. Wu and C. Bubeck, *Macromolecules*, 2013, **46**, 3512–3518; (f) J. T. Korhonen, T. Verho, P. Rannou and O. Ikkala, *Macromolecules*, 2010, **43**, 1507–1514; (g) S. Wu, S. Duan, Z. Lei, W. Su, Z. Zhang, K. Wang and Q. Zhang, *J. Mater. Chem.*, 2010, **20**, 5202–5209.
- 43 Y. S. Lu, Y. C. Lin and S. W. Kuo, *Macromolecules*, 2012, **45**, 6547–6556.
- 44 M. G. Mohamed, F. H. Lu, J. L. Hong and S. W. Kuo, *Polym. Chem.*, 2015, **6**, 6340–6350.
- 45 M. G. Mohamed, C. H. Hsiao, F. Luo and S. W. Kuo, *RSC Adv.*, 2015, **5**, 45201–45212.
- 46 H. Ren, D. Chen, Y. Shi, H. Yu and Z. Fu, *Polym. Chem.*, 2015, **6**, 270–277.
- 47 K. R. Scheule, F. Cardinaux, T. G. Taylor and A. H. Scheraga, *Macromolecules*, 1976, **9**, 23–33.
- 48 (a) J. Vappavuori, A. Priimagi and M. Kaivola, *J. Mater. Chem.*, 2010, **20**, 5260–5264; (b) J. D. Barrio, E. Blasco, L. Oriol, R. Alcalá and C. S. Somolinos, *J. Polym. Sci., Part A: Polym. Chem.*, 2013, **51**, 1716–1725.
- 49 A. H. Hofman, Y. Chen, G. T. Brinke and K. Loos, *Macromolecules*, 2015, **48**, 1554–1562.
- 50 T. J. Korhonen, T. Verho, P. Rannou and O. Ikkala, *Macromolecules*, 2010, **43**, 1507–1514.
- 51 J. Gao, N. Y. He, F. Liu, X. Zhang, Q. Z. Wang and G. X. Wang, *Chem. Mater.*, 2007, **19**, 3877–3881.
- 52 E. Y. Khoury, R. Hielscher, M. Voicescu, T. Gross and P. Hellwig, *Vib. Spectrosc.*, 2011, **55**, 251–258.
- 53 Y. S. Lu and S. W. Kuo, *RSC Adv.*, 2015, **5**, 88539–88547.
- 54 S. Jeon, J. Choo, D. Sohn and S. N. Lee, *Polymer*, 2001, **42**, 9915–9920.
- 55 J. Hwang and T. J. Deming, *Biomacromolecules*, 2001, **2**, 17–24.
- 56 N. J. Greenfield, *Nat. Protoc.*, 2006, **1**, 2876–2890.
- 57 C. Toniolo, A. Polese, F. Formaggio, M. Crisma and J. Kamphuis, *J. Am. Chem. Soc.*, 1969, **118**, 2744–2745.
- 58 Y. C. Lin, P. I. Wang and S. W. Kuo, *Soft Matter*, 2012, **8**, 9676–9684.
- 59 N. J. Greenfield and G. D. Fasman, *Biochemistry*, 1969, **8**, 4108–4116.
- 60 G. Holzwarth and P. Doty, *J. Am. Chem. Soc.*, 1965, **87**, 218–228.
- 61 (a) R. W. Woody, *Biopolymers*, 1978, **17**, 1451–1467; (b) A. K. Chen and R. W. Woody, *J. Am. Chem. Soc.*, 1971, **93**, 29–37; (c) K. Watanabe, K. Muto and T. Ishii, *Biospectroscopy*, 1997, **3**, 103–111.
- 62 M. C. Luyten, G. O. R. A. van-Dkenstein, G. ten-Brinke, J. Ruokolainen, O. Ikkala, M. Torkkeli and S. Serimaa, *Macromolecules*, 1999, **32**, 4404–4410.

- 63 S. Guo, K. Matsukawa, T. Miyata, T. Okubo, K. Kuroda and A. Shimojima, *J. Am. Chem. Soc.*, 2015, **137**, 15434–15440.
- 64 F. P. Nicoletta, D. Cupelli, P. Formoso, G. D. Filpo, V. Colella and A. Gugliuzza, *Membranes*, 2012, **2**, 134–197.
- 65 T. Y. Lai, C. Y. Cheng, W. Y. Cheng, K. M. Lee and S. H. Tung, *Macromolecules*, 2015, **48**, 717–724.
- 66 (a) C. W. Huang, P. W. Wu, W. H. Su, C. Y. Zhu and S. W. Kuo, *Polym. Chem.*, 2016, **7**, 795–806; (b) B. Tylkowski, S. Peris, M. Giamberini, R. Carcia-Valls, J. A. Reina and J. C. Ronda, *Langmuir*, 2010, **26**, 14821–14829; (c) G. S. Kumar and D. C. Neckers, *Chem. Rev.*, 1989, **89**, 1915–1925.